Accepted Manuscript

Chitosan-iron oxide nanocomposite based electrochemical aptasensor for determination of Malathion

Nirmal Prabhakar, Himkusha Thakur, Anu Bharti, Navpreet Kaur

PII: S0003-2670(16)30939-4

DOI: 10.1016/j.aca.2016.08.015

Reference: ACA 234745

To appear in: *Analytica Chimica Acta*

Received Date: 11 June 2016

Revised Date: 29 July 2016

Accepted Date: 9 August 2016

Please cite this article as: N. Prabhakar, H. Thakur, A. Bharti, N. Kaur, Chitosan-iron oxide nanocomposite based electrochemical aptasensor for determination of Malathion, *Analytica Chimica Acta* (2016), doi: 10.1016/j.aca.2016.08.015.

Graphical Abstact:

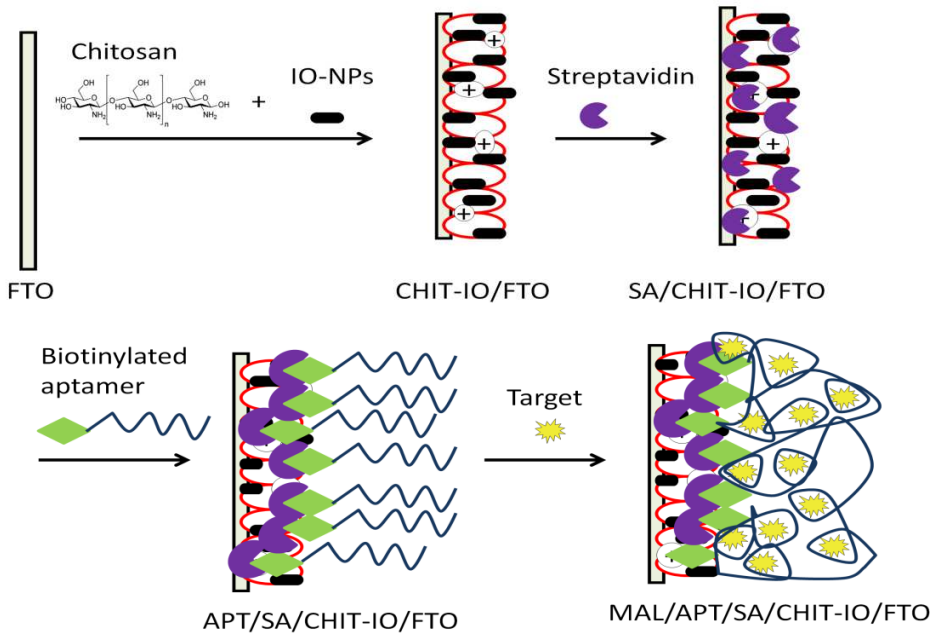

Chitosan-iron oxide nanocomposite based electrochemical aptasensor for determination of Malathion

Nirmal Prabhakar*, Himkusha Thakur, Anu Bharti, Navpreet Kaur

Department of Biochemistry, Panjab University, Chandigarh (India)-160014

*Corresponding Author: nirmalprabhakar@gmail.com, nirmalprabhakar@pu.ac.in

A B S T R A C T

An electrochemical aptasensor based on chitosan-iron oxide nanocomposite (CHIT-IO) film deposited on fluorine tin Oxide (FTO) was developed for the detection of malathion. Iron oxide nanoparticles were prepared by co-precipitation method and characterized by Transmission electron microscopy and UV-Visible spectroscopy. The biotinylated DNA aptamer sequence specific to the malathion was immobilized onto the iron oxide doped-chitosan/FTO electrode by using streptavidin as linking molecule. Various characterization studies like Field Emission-Scanning Electron Microscopy (FE-SEM), Fourier Transform Infrared Spectroscopy (FT-IR), and Electrochemical studies were performed to attest the successful fabrication of bioelectrodes. Experimental parameters like aptamer concentration, response time, stability of apaelectrode and reusability studies were optimized. Aptamer immobilized chitosan-iron oxide nanocomposite (APT/SA/CHIT-IO/FTO) bioelectrodes exhibited LOD of about 0.001ng/mL within 15 minutes and spike-in studies revealed about 80-92% recovery of malathion from the lettuce leaves and soil sample.

Keywords: Electrochemical biosensor, Chitosan-iron oxide nanocomposite, Aptamer, Malathion Organophosphates

1. Introduction

Pesticides are widely used in agriculture as high efficiency insecticide to preserve the crops from pests which has raised serious health concern. Neurotoxic effects of pesticides are hazardous to both human health and the environment. Pesticides are either carcinogenic or cytotoxic and are responsible for many respiratory diseases [1]. Organophosphates (OPs) contribute about 38% of the total pesticide used worldwide [2]. Malathion, Parathion, Methyl-parathion, Chlorpyrifos, Diazinon and Phosmet are mostly used OP pesticides. The Malathion (S-1,2-bis(ethoxy carbonyl) ethyl O,O-dimethyl phosphorodithionate) has been extensively used to control a variety of insects in both urban and agricultural field [3]. Malathion leads to the inhibition of acetylcholinesterase activity resulting in the interference of normal neuronal functioning and sometimes fatal [4,5]. Thus, for the determination of these toxic compounds various analytical methods are required to ensure safety of human health and environment. Conventional methods commonly used for the detection of OPs are gas-chromatography (GC) [6], high performance liquid chromatography (HPLC) [7], mass spectrometry [8], enzyme-linked immunosorbent assay (ELISA) [9], capillary electrophoresis [10] and various other spectrophotometric methods [11]. These methods are sensitive but are time consuming, expensive, require expertise and having low limits of detection. Therefore, there is urgent need for the development of such a method with rapidity, selectivity, reliability and low cost instrumentation. Biosensors exhibit exceptional performance capabilities like high sensitivity and specificity, rapid response, low cost, portability, relatively compact size, user friendly operation and continuous real time analysis. Inhibition of acetylcholinesterase (AChE) based biosensors have been widely used for the determination of OPs [12,13,14,15]. These sensors can be used for a wide range of organophosphates and carbamate detection due to inhibiting action

on AChE and thus lack specificity but are ideal for initial screening of the samples for presence of OPs and carbamates. Thus less stability due to loss of bioactivity by denaturation and lack of specificity discourage the researchers and compel to explore novel biomolecule that may circumvent these limitations.

Aptamer have been used as biological recognition elements to develop efficient aptasensor allowing the specific detection of malathion. Aptamers are DNA or RNA sequences selected in vitro from oligonucleotides libraries to specific target molecules. Aptamer exhibit competitive advantages over other biorecognition molecules such as remarkable target diversity, specificity, synthesis, convenience tight-binding capability, chemical stability and flexibility of chemical modification for labeling or favorable immobilization. They are thermally stable, reusable and can be easily modified for their detection and immobilization by introduction of reporter molecules and functional groups [16,17].

Among all the transduction approaches, electrochemical detection is an attractive sensing platform in the field of biosensors [18-21]. However, since last few years, electrochemical transduction has received much attention to monitor the behavior of target-aptamer complex on electrode surface [22-24]. This sensing methodology has various advantages including simplicity, rapidity, low cost and high sensitivity. Presently, nanoparticles are being used to improve the analytical performance of electrochemical biosensors for chemical and biological sensing [25]. Metal oxide nanoparticles such as iron oxide [26,27], zinc oxide [28], cerium oxide [29] have been suggested as promising matrices for the sensing application of desired biomolecules. Iron oxide nanoparticles attracted much attention as an electrochemical transducer because of their ability to enhance conductivity, super paramagnetism, signal amplification and favorable microenvironment for protein adhesion thus improving sensitivity and selectivity.

However, the problem of aggregation and rapid biodegradation of iron oxide nanoparticles (IONPs) onto a given matrix containing biomolecules can be overcome by dispersing IONPs in a biopolymer matrix of chitosan (CHIT) to make them suitable for biosensor applications. CHIT has gained growing interest due to its biocompatibility and biodegradability over the other polymers. Also, owing to the presence of -OH and -NH_2 groups on CHIT provides flexibility to material with specific functionality [30]. Recently, fluorine tin Oxide (FTO) glass sheets are gaining wide attention as solid support in the development of electrochemical biosensors [31]. FTO sheets are known to exhibit high electrical conductivity, relative stability under atmospheric conditions, chemical inertness, mechanical strength, visible transparency and resistance at high temperature. Furthermore, FTO sheets are cost effective and eliminate the problem of diffusion as seen in case of ITO sheets.

Here we report the electrochemical aptasensor based on iron oxide doped chitosan deposited onto fluorine doped tin oxide (FTO) coated glass plates for determination of malathion.

2. Materials and methods

2.1. Materials

Biotinylated Aptamer sequence (72 mer), Malathion, Streptavidin and fluorine-doped tin oxide (FTO) sheets were purchased from Sigma-Aldrich (India). Chitosan, ferrous chloride tetrahydrate and ferric chloride hexahydrate were purchased from HiMedia Laboratories Pvt. Ltd. Mumbai, India. Autoclaved buffer solutions were used in experiments. The Stock solution of 100mM *N*-[3-(dimethylaminopropyl)-*N*-3-ethylcarbodiimide hydrochloride] (EDC), 100 mM *N*-hydroxysuccinimide (NHS) and stock solution of 50 μg/mL streptavidin in PBS (pH 7.5) were

prepared. All other chemicals used were of analytical grade. The deionized water has been used throughout the experiment. Aptamer sequence specific to malathion was taken from the previously reported literature by Barahona et al. [32].

Biotinylated Aptamer Sequence-

5'(Btn)ATCCGTCACACCTGCTCTTATACACAATTGTTTTTCTCTTAACTTCTTGACTGC-TGGTGTTGGCTCCCGTAT-3'.

2.2. Preparation of iron oxide nanoparticles (IONPs) and characterization

Iron Oxide nanoparticles were synthesized using chemical co-precipitation method [33] and were stored in desiccator for future use after drying. The synthesized IONPs were characterized using Transmission electron microscopy (TEM) [Hitachi(H-7500)] and UV-Visible spectroscopy [Shimadzu UV-1800].

2.3. Fabrication of aptaelectrodes and characterization studies

A suspension was prepared by dissolving IO nanoparticles (50 mg) in distilled water (10 mL) and sonicated for 1 hr at room temperature. This suspension was mixed with CHIT solution (solution prepared by dissolving 3 g of chitosan in 1% acetic acid solution and ultra-sonicated at RT for 1hr till the solution became transparent) and kept at stirring for 5 hr. The electrodes were prepared by dip coating the FTO sheets in CHIT-IO hybrid nanocomposite suspension. The prepared CHIT-IO electrodes were coated with activated streptavidin solution. For activation, 20 µL of streptavidin (0.5 mg/mL) was dissolved in mixed solution of EDC (10 mM) and NHS (15 mM) and kept at room temperature for 3 hr. These streptavidin immobilized CHIT-IO hybrid nanocomposite films were kept in humid chamber in 4ºC overnight at and rinsed with deionized

water to remove any unbound molecules. The biotinylated single stranded (ss) DNA aptamer (15 µM) was immobilized on the surface of the modified electrode (SA/CHIT-IO) via biotin-streptavidin interaction for 12 hr at 4ºC in humid chamber and rinsed with deionized water to remove any unbound aptamer from the bioelectrode surface (Scheme 1). The EDC-NHS activated -COOH group of streptavidin forms covalent bond with the -NH_2 groups present in CHIT in CHIT-IO/FTO electrode. The further immobilization of biotinylated aptamer onto streptavidin attached CHIT-IO nanocomposite (SA/CHIT-IO/FTO) takes place via strong biotin-streptavidin interaction.

All the electrodes (CHIT/FTO, CHIT-IO/FTO, SA/CHIT-IO/FTO and APT/SA/CHIT-IO) were characterized by Fourier Transform Infrared Spectroscopy (FT-IR) [Nicolet 1S50 FT-IR], Electrochemical studies (Differential Pulse Voltammetry (DPV) and Electrochemical Impedance Spectroscopy) [Potentiostat/Galvanostat, AutoLab EcoChemie, Netherlands] and Field Emission-Scanning Electron Microscopy (FE-SEM) [Jeol-JSM-6100] to affirm the successful fabrication of bio-electrodes.

For the fabrication of aptaelectrodes, the concentration of aptamer to be immobilized was optimized using a range from 2-20 µM aptamer. The aptaelectrodes were prepared by immobilizing different concentration on the SA/CHIT-IO/FTO electrode for 12 hr in a humid chamber at 4ºC and response was recorded electrochemically. Another optimization was done with respect to the incubation time from 5 min to 20 min with the target (malathion) stating the time required for the aptaelectrode to generate a response with the target (Supplementary data).

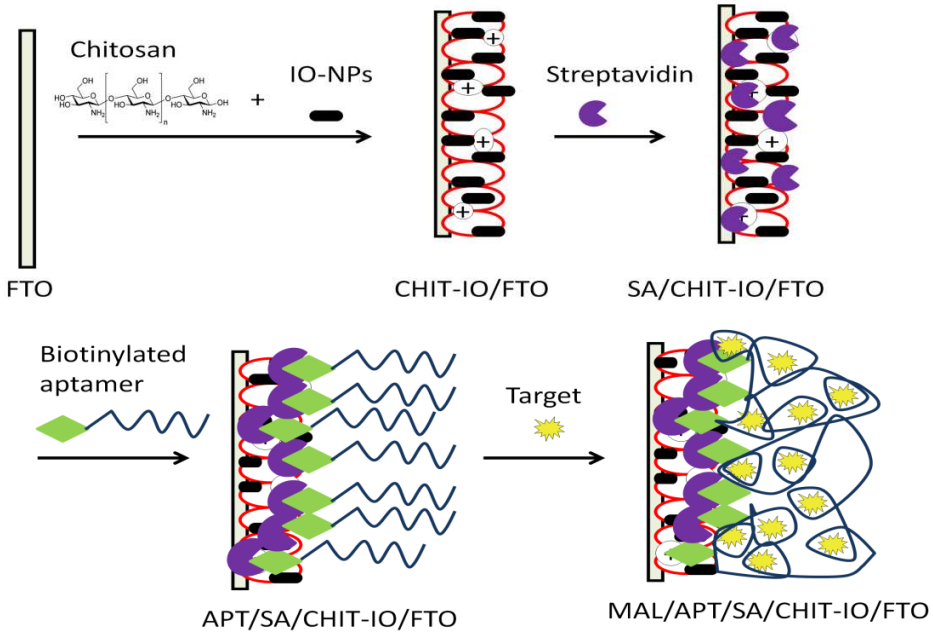

Scheme. 1. Schematic illustration for the fabrication of working aptaelectrode.

2.4. Response studies

For the detection studies, 15 µM aptamer was immobilized for 12 hr on the SA/CHIT-IO electrode surface. The aptaelectrode was incubated with malathion concentrations range from 0.01µg/mL, - 0.001ng/mL) for 15 min and response was studied with DPV taken in 0.05M PBS (pH 7.0, 0.9% NaCl) containing 5 mM $[Fe(CN)_6]^{3-/4-}$ at a potential range 0.2-0.7 V with a scan rate of 100 mV/s.

2.5. Stability and reusability of the aptaelectrodes

The stability of aptaelectrode was studied upto 28 days (stored at 4ºC) at the interval of 7days by DPV studies. To regenerate the aptaelectrode, 10 mL of 50mM NaOH solution was applied on the surface of APT/SA/CHIT-IO electrode for 10 min. The reusability of the biosensor was tested by repetitive detection of the target after regeneration every time till the current response reaches a non-significant value.

2.6. Spike-in studies (Lettuce leaves and soil sample)

Lettuce leaves sample:- 1g of leaf sample was incubated with four different concentration (0.01µg/mL, 0.0025µg/mL, 0.005ng/mL and 0.001ng/mL) of malathion for 2 hr at room temperature. Leaf samples were homogenized by adding solution of acetone (1mL) and 0.1M PBS (1mL), thereafter centrifuged for 20 min at 2000 rpm. Supernatant containing malathion was used for further sensing studies using aptaelectrode.

Soil sample:- 2g of soil sample was dissolved in 50mL of deionized H_2O. And the solution was spiked with different concentrations (0.01µg/mL, 0.0025µg/mL, 0.005ng/mL and 0.001ng/mL) of malathion. This spiked sample was then used for electrochemical measurements using APT/SA/CHIT-IO electrode.

3. Results and discussions

3.1. Characterization of IONPs

The presence of dark round spots in TEM image (Fig. 1A) clearly highlights the formation of reasonably uniform sized IONPs powder with less than diameter of 20 nm. The UV-VIS spectrum (Fig. 1B) of IONPs showed an absorption peak at 359 nm due to surface plasmon resonance [34]. According to Mallick et al. the absorption bands appeared in region I

(250-400nm) are due to the ligand-to-metal charge-transfer (LMCT) transitions (direct transitions) with combined contributions from the Fe^{3+} ligand field transitions [35].

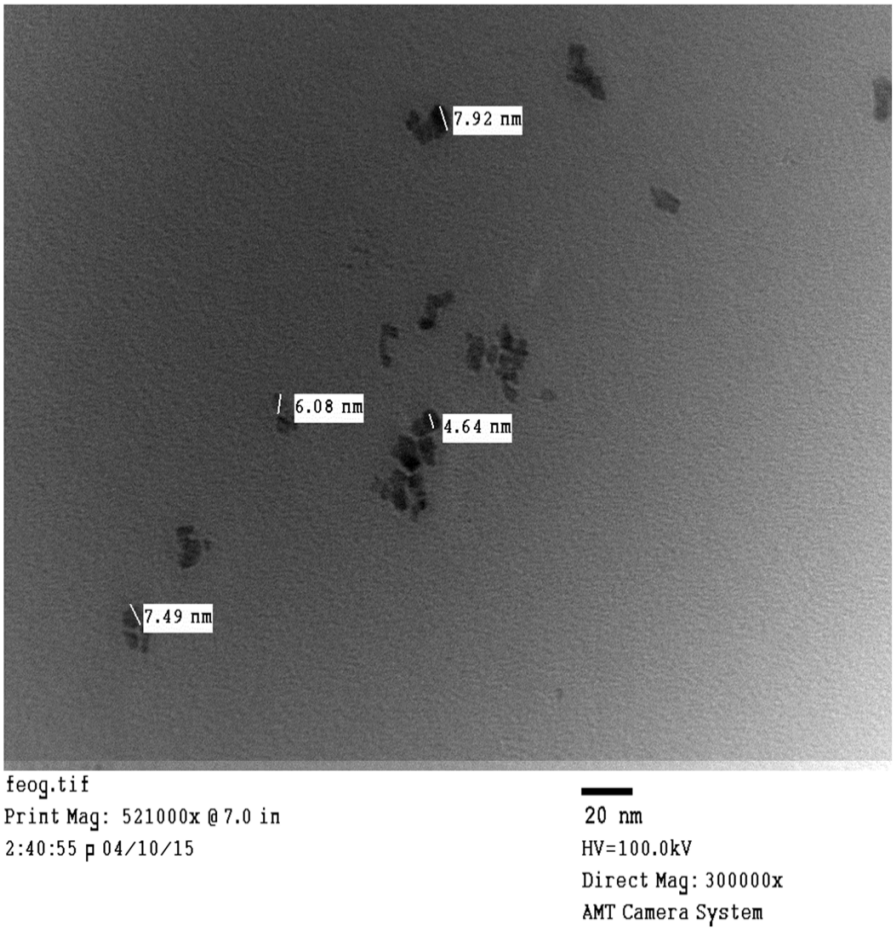

(A)

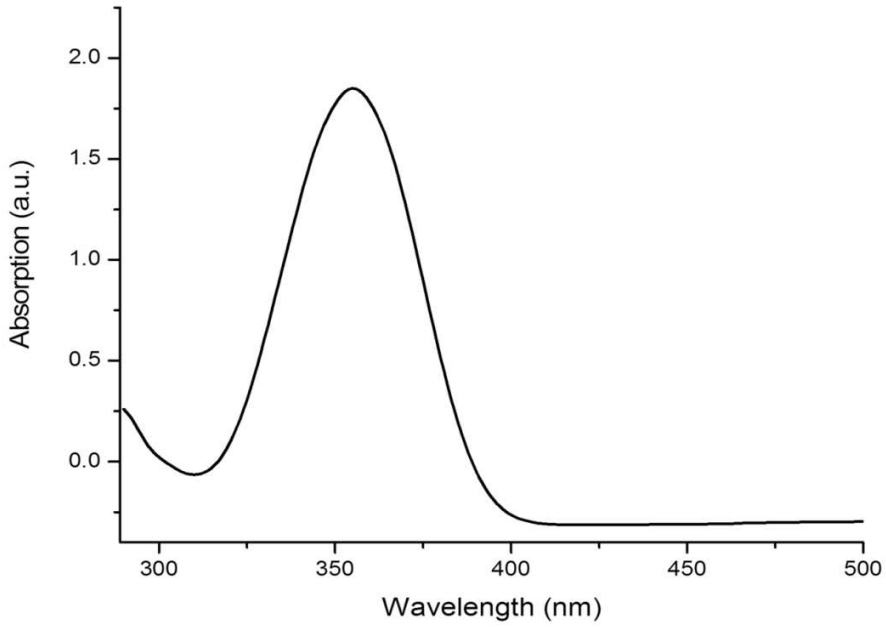

(B)

Fig. 1. Characterization studies of Iron oxide nanoparticles: **(A)** TEM image, **(B)** UV-VIS spectrum.

3.2. Characterization studies

3.2.1. FT-IR studies

Fig. 2 shows the FT-IR spectra of (a) CHIT/FTO (b) CHIT-IO/FTO (c) SA/CHIT-IO/FTO and APT/SA/CHIT-IO/FTO (d) to verify the hybrid nanocomposite as well as fabrication of bioelectrodes. The FT-IR spectra of bare chitosan (Fig. 2a) displayed a broad band at 3366 cm^{-1} due to the stretching vibration mode of -OH and $-NH_2$ group. The band in the region 2956 cm^{-1} was attributed to the $-CH_3$ and $-CH_2$ groups, that led to chitosan symmetric and antisymmetric stretching modes. The band at 1640 cm^{-1} was due to amide I group (C-O

stretching along with N-H deformation mode), 1545 cm^{-1} peak was attributed to the -NH_2 group, 1458 cm^{-1} peak was due to C-N axial deformation, 1150 cm^{-1} was assigned to broad peak of β (1-4) glycosidic bond in the polysaccharide unit and 1038 cm^{-1} to the stretching vibration of C-O-C in glucose circle [36]. The IR corresponding to -NH/-OH stretching modes in bare chitosan were found to be shifted in the spectra of CHIT-IO hybrid nanocomposite film (curve b). It appeared that amine groups of chitosan bound with IONPs via electrostatic interaction. The IR-band corresponding to curve b shifted to lower wavenumber due to the formation of a complex between surface charged IONPs and cationic chitosan matrix, indicating the formation of CHIT-IO hybrid nanocomposite. Also the characteristic peaks displayed by CHIT-IO (Fig. 2b) had decreased intensities than CHIT (Fig. 2a) because amide group of chitosan was involved in the formation of nanocomposite with IONPs [37].

In FTIR spectrum of SA/CHIT-IO/FTO bioelectrode, the IR bands corresponding to the -NH and -OH band were further shifted to lower wave number (3276 cm^{-1}) corresponding to CHIT-IO (3317cm^{-1}) hybrid. This suggests that amine (-NH) groups of chitosan were also involved in the interaction with carboxyl (-COO^-) group of streptavidin biomolecule. The absorption bands of amide I group at 1610-1690 cm^{-1} represent the C=O stretching vibration of peptide linkages and amide II group at 1500-1600 cm^{-1} from a combination of N-H bending and C-N stretching. The FT-IR spectrum of SA/CHIT-IO/FTO bioelectrode (Fig. 2c) showed two absorption peak at 1620 cm^{-1} and 1523 cm^{-1}, which corresponded to the amide I and amide II groups of the protein on CHIT-IO/FTO nanocomposite surface [38]. After the immobilization of aptamer onto SA/CHIT-IO/FTO bioelectrode, the absorption bands corresponding to base pairs and phosphate backbone of Aptamer (DNA) were observed. The aptamer layer covered most of the functional groups that appeared in previous spectrum of SA/CHIT-IO/FTO bioelectrode (Fig.

2c), and thus those displayed broader peaks with less intensity in the spectrum of APT/SA/CHIT-IO/FTO aptaelectrode (Fig. 2d). The peak appeared at 1632 cm^{-1} was attributed to in-plane ring vibration of Thymine in ssDNA [39], while the peak at 1136 cm^{-1} showed the presence of sugar phosphate backbone of aptamer [40].

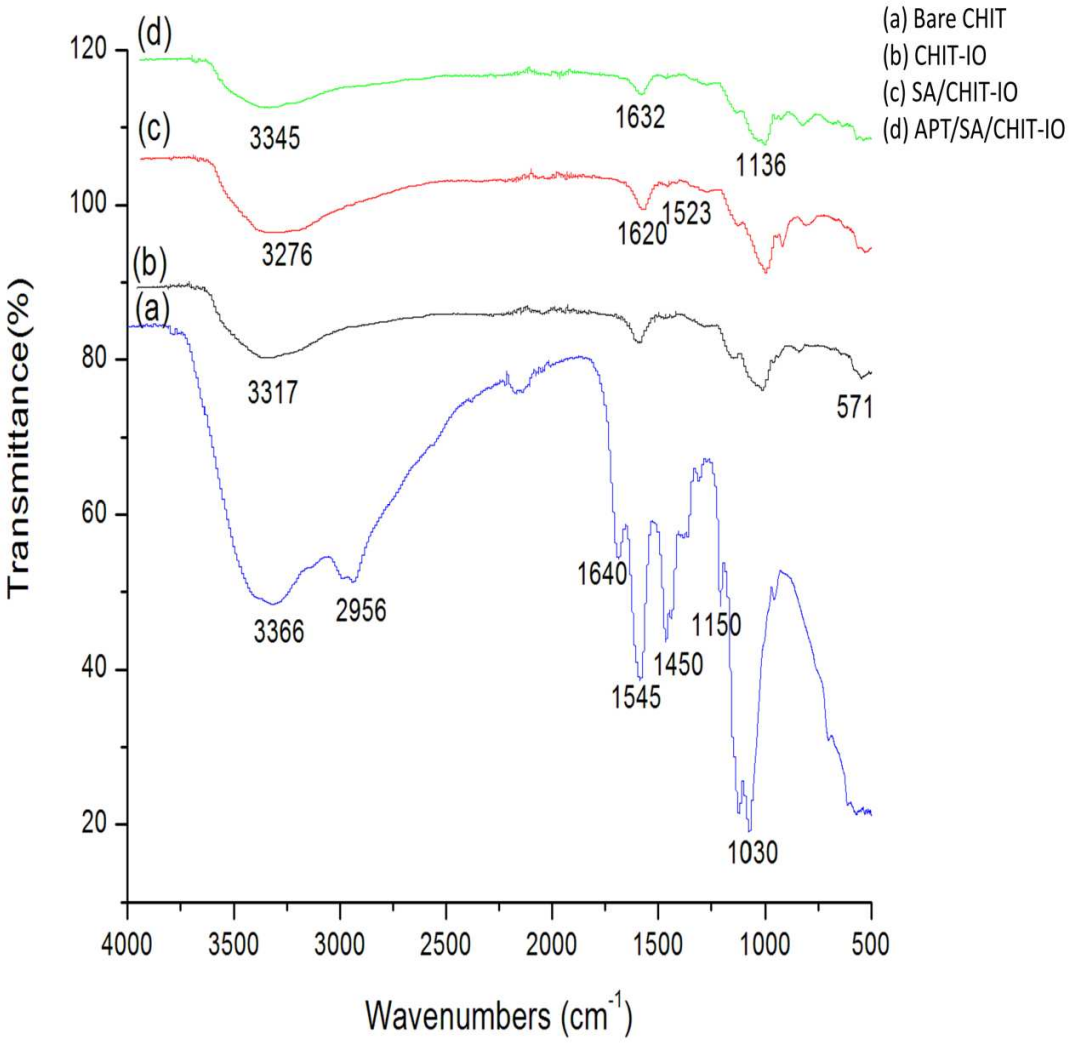

Fig. 2. FT-IR spectra of (a) CHIT/FTO (b) CHIT-IO/FTO (c) SA/CHIT-IO/FTO (d) APT/SA /CHIT-IO/FTO.

3.2.2. FE-SEM studies

Surface morphological studies of prepared nanocomposite films and aptaelectrodes were characterized by FE-SEM images as shown in Fig. 3. The FE-SEM image of CHIT (Fig. 3A) was a porous surface representing its polymeric nature. In Fig. 3B, the globular porous microstructure seen after the incorporation of IONPs into CH indicates the synthesis of CH-IO nanocomposite. This may indicate the electrostatic interactions between cationic -CH and anionic IONPs [41]. Fig. 3C shows the globule like structures of streptavidin covering the CH-IO matrix. In Fig. 3D, a uniform immobilization of the aptamer on the surface of CHIT-IO/FTO film can be observed.

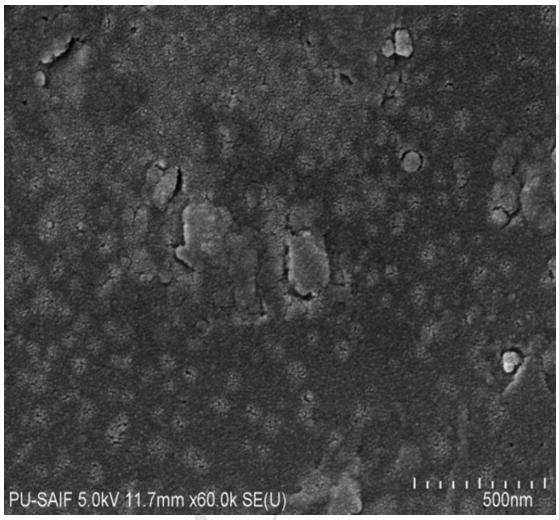

(**A**)

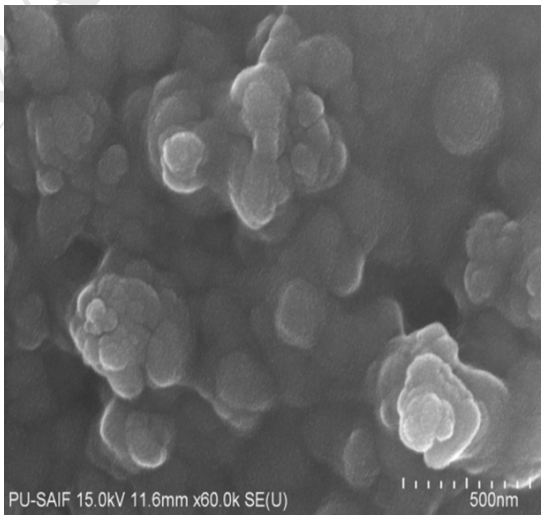

(B)

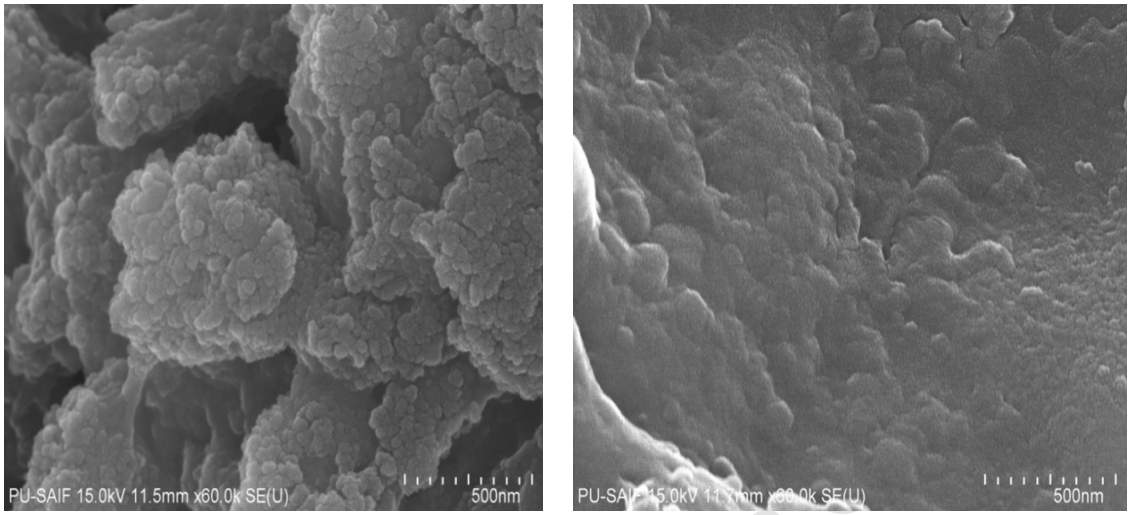

(C) **(D)**

Fig. 3. FE-SEM images **(A)** CHIT/FTO **(B)** CHIT-IO/FTO **(C)** SA/CHIT-IO/FTO **(D)** APT/SA/ CHIT-IO/FTO.

3.2.3. Electrochemical studies

Fig. 4(A) shows the results of the DPV measurements carried out on CHIT/FTO film (i), CHIT-IO/FTO nanocomposite (ii), SA/CHIT-IO/FTO bioelectrode (iii) APT/SA/CHIT-IO/FTO (iv) and MAL/APT/SA/CHIT- IO/FTO aptaelectrode. The DPV curve of pure CHIT/FTO electrode (Fig. 4(A), curve i) showed the lowest peak of current suggesting weak conductivity of bare chitosan. However, in Fig. 4(A), curve (ii) a significant increase in the magnitude of current response was observed on addition of iron oxide NPs. This might be attributed to the presence of IONPs resulting in enhanced adsorption of the redox moieties on cationic CHIT-IO/FTO nanocomposite surface with improvement in electron transfer and electrical conductivity. With the binding of activated streptavidin (SA) onto CHIT-IO/FTO surface (Fig. 4(A), curve iii) there was a decrease in the magnitude of current peak revealing inhibition of the electron transfer and hence less electrical conductivity. The DPV curve of APT/SA/CHIT-IO/FTO (Fig. 4(A), curve

iv) showed an increase in peak current as compared to that of SA/CHIT-IO/FTO bioelectrode, because the electrical characteristics of aptamer resulted in increased number of charge carriers and enhanced electron transfer towards the electrode [42]. Curve (v) the DPV image of APT/SA/CHIT-IO/FTO aptaelectrode in response to malathion showed a decrease in peak of current as compared to the aptaelectrode (curve iv) due the formation of aptamer target complex which hindered the diffusion of $[Fe(CN)_6]^{3-/4-}$ towards the electron surface.

The Nyquist plots of EIS studies of CHIT/FTO, CHIT-IO/FTO, SA/CHIT-IO/FTO, APT/SA/CHIT-IO/FTO and MAL/APT/SA/CHIT-IO/FTO electrodes are shown in Fig. 4(B) in 0.05M PBS (pH 7.0, 0.9% of NaCl) containing 5mM of$[Fe(CN)_6]^{3-/4-}$. There was a significant increase in the diameter of semicircle for CHIT (R_{ct} =1000Ω) as compared to that of CHIT-IO nanocomposite suggesting increased flow of electrons after addition of iron-oxide nanoparticles (R_{ct} decreases to 500Ω). After the SA immobilization, there was increase in diameter of semicircle of CHIT-IO (R_{ct} =900Ω) due to presence of non-conducting protein causing hindrance in electron flow. The nyquist curve for APT/SA/CHIT-IO showed a decrease in the diameter and R_{ct} value (700Ω) as compared to SA/CHIT-IO that could be due to the negative backbone of DNA aptamer, responsible for the conductivity of electrode. When malathion was immobilized on aptaelectrode the diameter further increased and R_{ct} value was 800Ω because of the intereference in the electron flow.

The electron transfer rate constant (k_{cr}) was calculated using following equation [27]:

$$k_{cr} = RT/n^2F^2AR_{ct}[S] \qquad \text{equation 1}$$

where R= gas constant, T= absolute temperature, F= faraday constant, A= electrode area, S= bulk concentration of redox probe and n= number of transferred electrons per molecule of the redox probe. The value of k_{cr} for bare CHIT was noted as (0.53×10^{-7} cm/s), which increased

twice upon the addition of IONPs (1.06 $\times 10^{-7}$ cm/s). The immobilization of streptavidin led to decrease in the k_{cr} value to 0.59 $\times 10^{-7}$ cm/s but aptamer binding again increased the value to 0.76 $\times 10^{-7}$ cm/s. The incubation of aptaelectrode with the target decreased the k_{cr} value again to 0.66 $\times 10^{-7}$ cm/s.

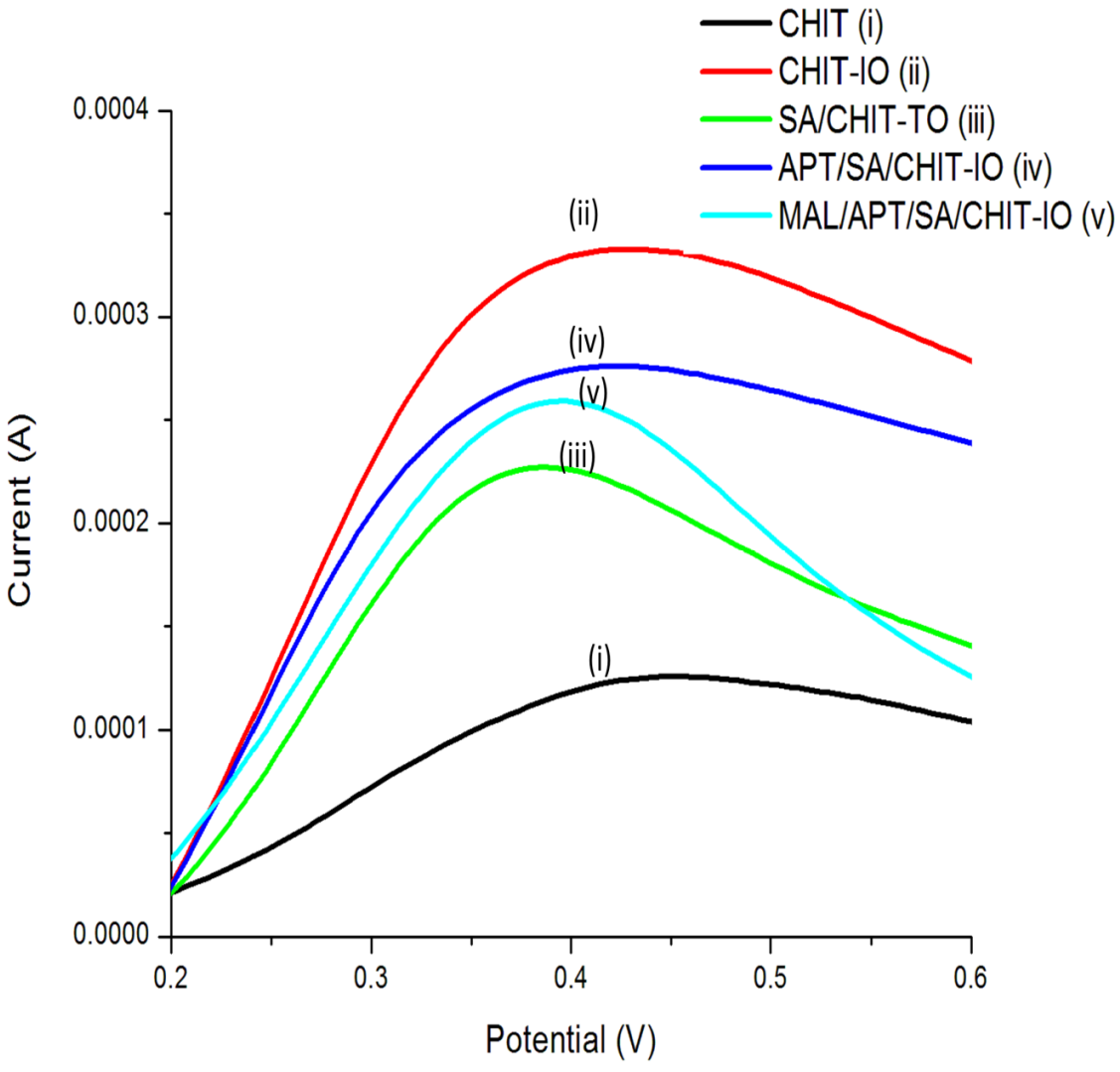

(A)

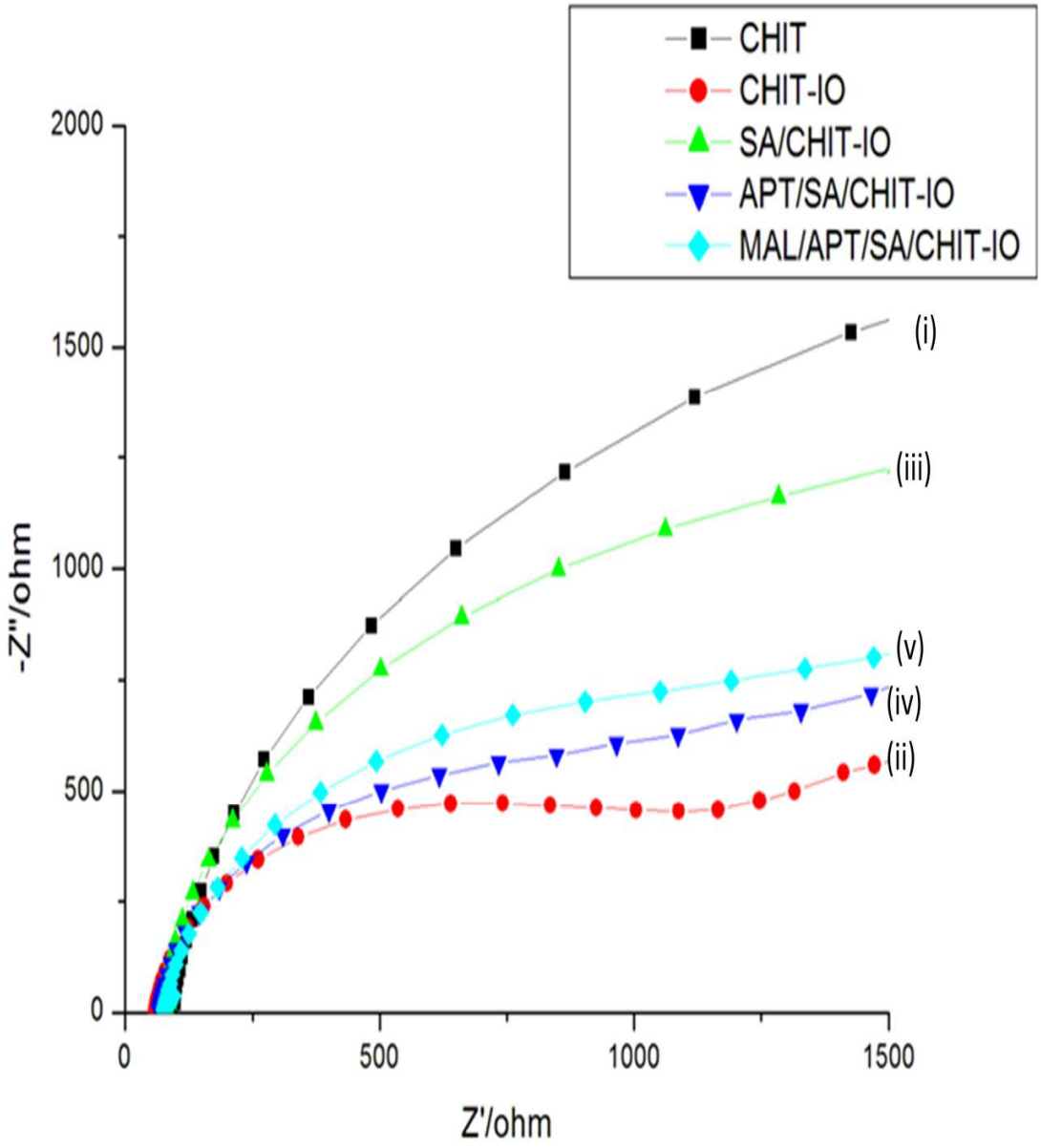

(B)

Fig. 4. (A) DPV studies of i) CHIT/FTO ii) CHIT-IO/FTO iii) SA/CHIT-IO/FTO iv) APT/SA/CHIT-IO/FTO v) MAL/APT/SA/CHIT-IO/FTO at potential range from 0.2 to 0.6 V with a scan rate of 100 mV/s. in 0.05M PBS (pH-7.0, 0.9% NaCl) containing 5mM $[Fe(CN_6)]^{3-/4-}$

and **(B)** EIS measurements of i) CHIT/FTO ii) CHIT-IO/FTO iii) SA/CHIT-IO/FTO iv)APT/SA/CHIT-IO/FTO v) MAL/APT/SA/CHIT-IO/FTO in 0.05M PBS (pH-7.0, 0.9% NaCl) containing 5mM $[Fe(CN_6)]^{3-/4-}$ within the frequency range 100 kHz-100 mHz.

3.3. Sensing studies

Fig. 5 (A) shows DPV response curves of aptaelectrodes after interaction with the malathion concentration ranging from 0.001 ng/mL to 0.01µg/mL for 15 min. As the concentration of malathion increased from 0.001 ng/mL to 0.01µg/mL, the DPV peak current of the aptaelectrode decreased due to the formation of more 3D-complex between aptamer with malathion that caused inhibition in flow of current. Hence, more the concentration of malathion, more the interference and more decrease in the current peak. 0.01µg/mL of malathion concentration was sufficient to saturate all the aptamer moieties present on aptaelectrode. Therefore, there was no more decrease in current above this concentration (0.01µg/mL). While, 0.001ng/mL was the least concentration that could bind to aptamer molecules and below this concentration, there was no increase in the peak current suggesting the low detection limit. A linear calibration curve (B) displayed the linear relationship between the peak current and malathion concentrations.

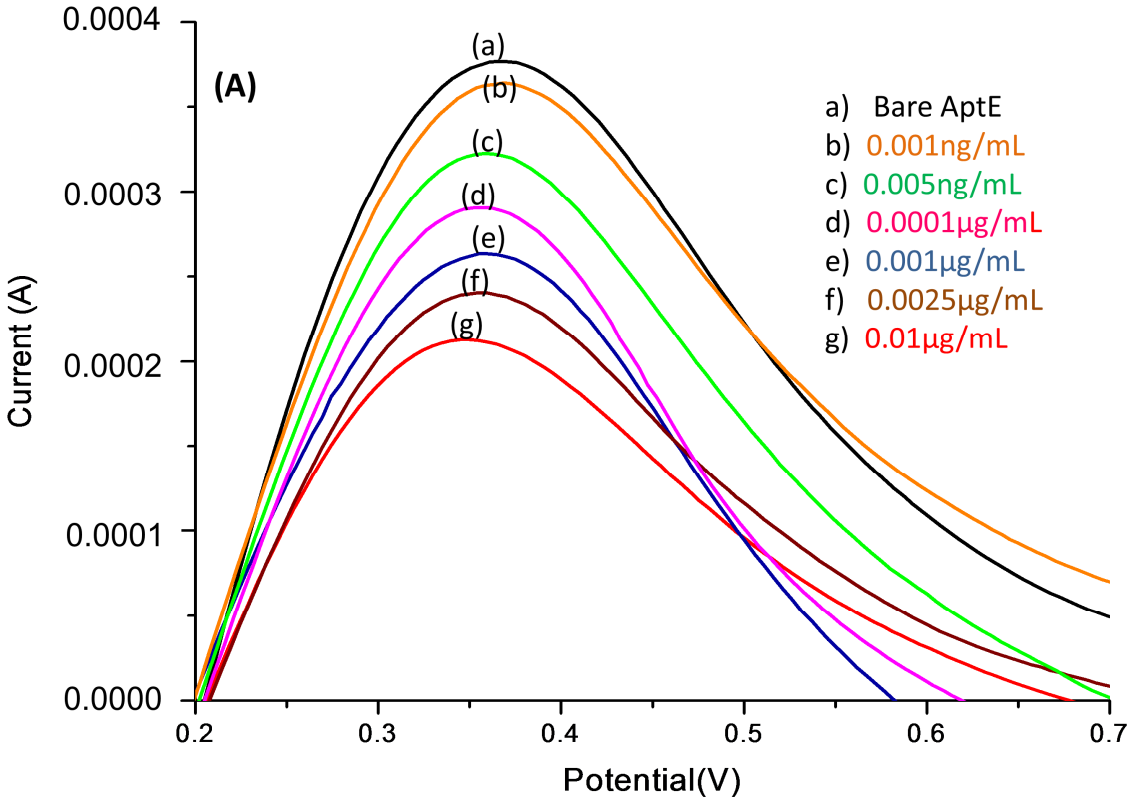
(A)
Current (A)
Potential(V)
0.0004
0.0003
0.0002
0.0001
0.0000
0.2
0.3
0.4
0.5
0.6
0.7
(a)
(b)
(c)
(d)
(e)
(f)
(g)
a) Bare AptE
b) 0.001ng/mL
c) 0.005ng/mL
d) 0.0001µg/mL
e) 0.001µg/mL
f) 0.0025µg/mL
g) 0.01µg/mL

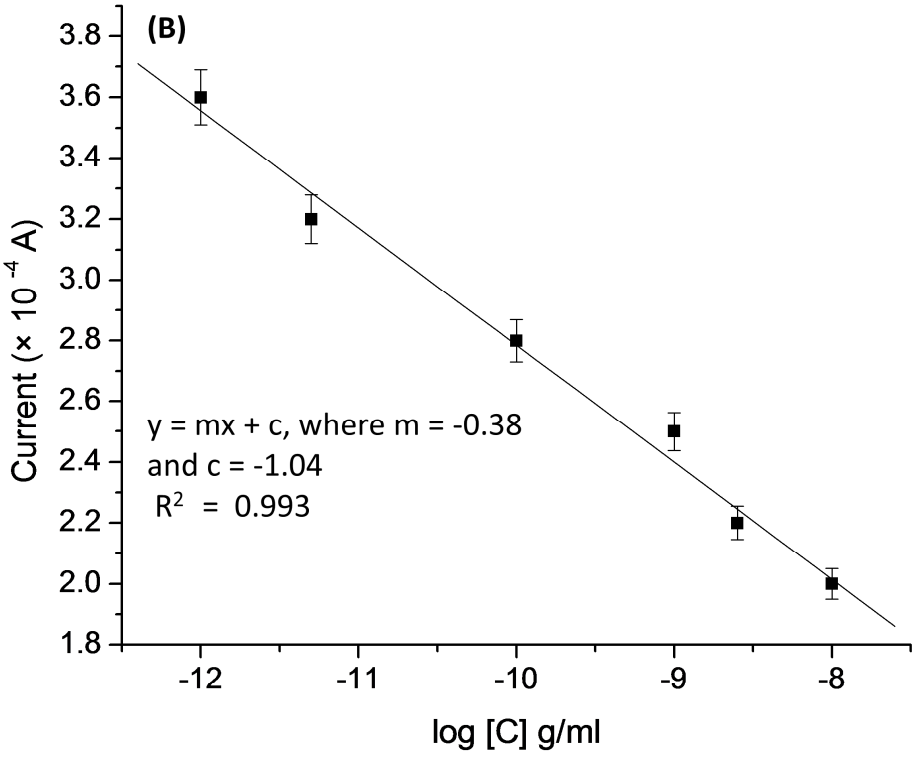

Fig. 5. DPV response of **(A)** aptaelectrode with different concentrations of malathion (a) Bare aptaelectrode (b) 0.001ng/mL (c) 0.005ng/mL (d) 0.0001µg/mL (e) 0.001µg/mL (f) 0.0025µg/mL (g) 0.01µg/mL; at potential range from 0.2 – 0.7 V with a scan rate of 100 mV/s in 0.05 M PBS (pH-7.0, 0.9% NaCl) containing 5mM $[Fe(CN)_6]^{3-/4-}$ and **(B)** shows the linear relationship between the peak current changes obtained by DPV and the logarithm of malathion concentrations. Error bars show the standard deviations of measurements taken from three independent experiments.

3.4. Stability and reusability studies of aptasensor

The aptaelectrodes were stored at 4^{0} C and the stability studies were performed for about thirty days. The response of the respective aptaelectrodes were analysed with the interval of fourteen

and then seven days. There was gradual decrease in the peak current from 0 day-28 day (Fig. 6A). The aptasensor retained about 81% of its original response at 14 day and decreased gradually to 79 % and 75% after 21days and 28days, respectively. This suggested that the aptasensor had relatively good stability of about half of month. The reusability (Ru) of the aptaelectrode was studied after regenerating it every time and noting down its electrochemical response with the target (malathion). The DPV showed the reduction in peak currents to 96%, 94%, 90%, 85% , 81%, 77% and 69%, from seven successive regenerations, indicating that the proposed aptaelectrode diplayed reusuability of 5 times (Fig. 6B).

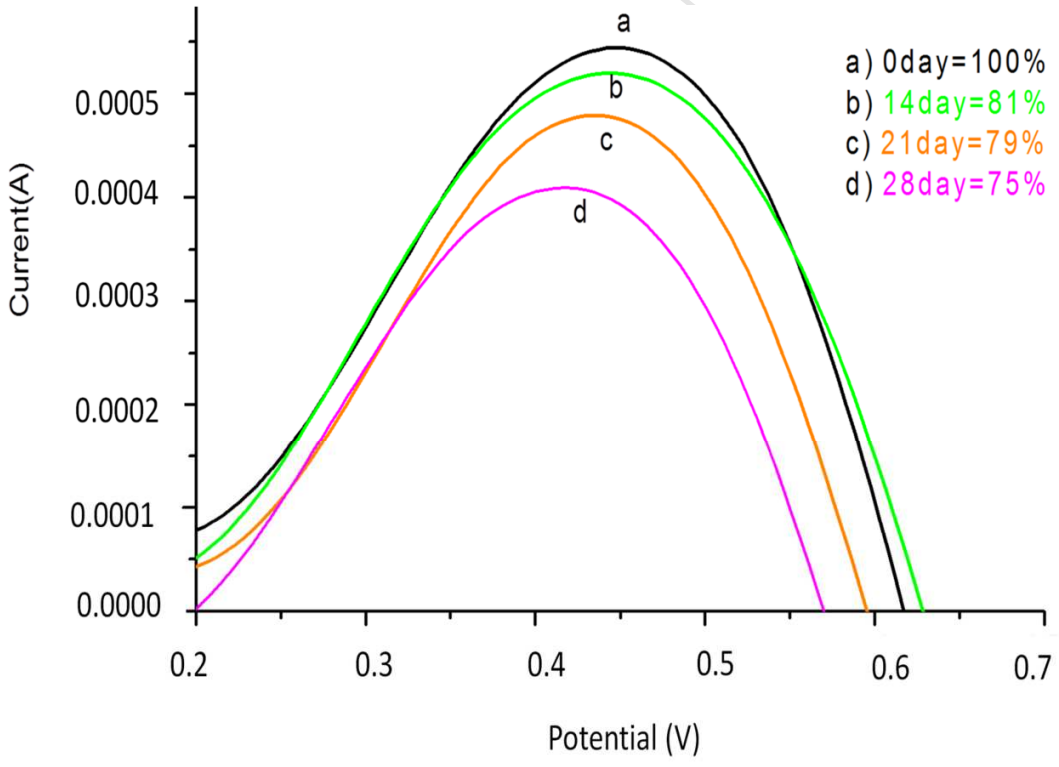

(A)

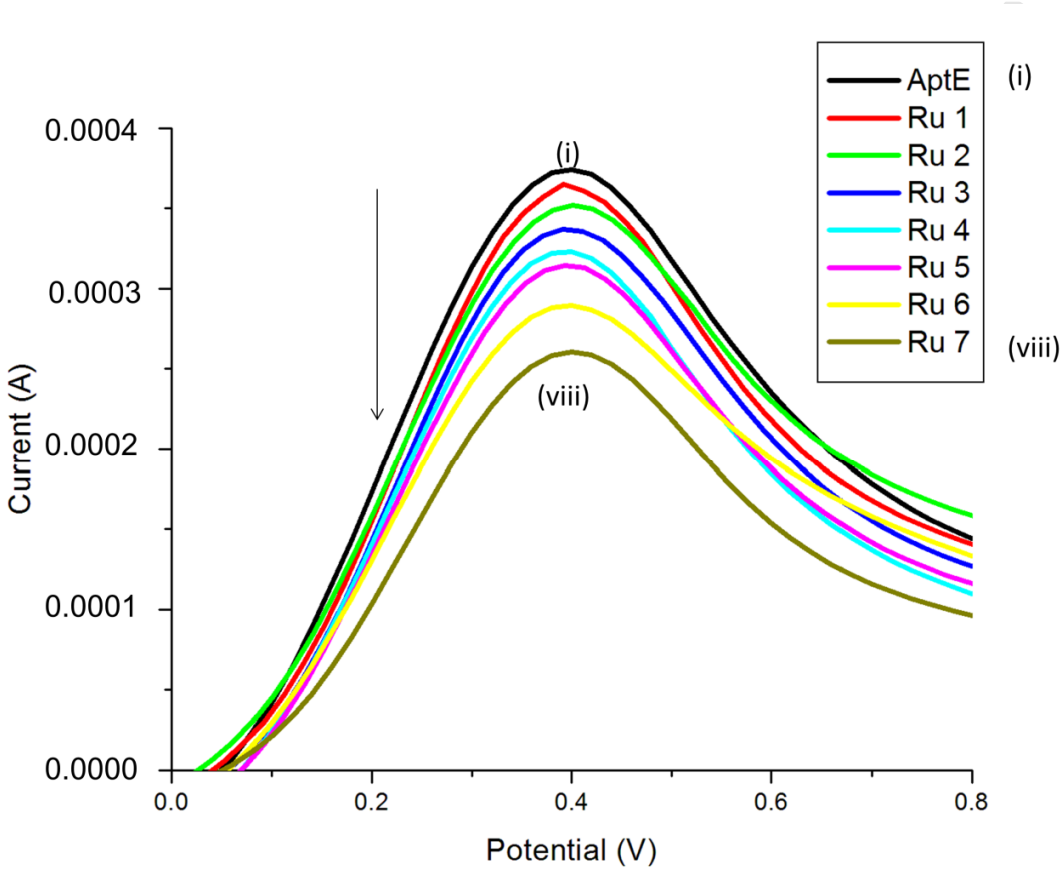

(B)

Fig. 6. DPV studies to evaluate (**A)** Stability of aptaelectrode with malathion a) 0 day b) 14 day c) 21 day d) 28 day; and **(B)** Regeneration with 50mM NaOH (a) Aptaelectrode (b) Ru 1 (c) Ru 2 (d) Ru 3 (e) Ru 4 (f) Ru 5 (g) Ru 6 (h) Ru 7; at potential range from 0.0 to 0.8 V with a scan rate of 100mV/s in 0.05 M PBS (pH-7, 0.9% NaCl) containing 5mM $[Fe(CN)_6]^{3-/4-}$.

3.5. Spike-in studies

To evaluate the performance of synthesized aptasensor in real samples, prepared lettuce sample and soil sample was applied onto the surface of aptaelectrode in triplicates. Recovery percentage obtained from the spiked in samples of lettuce leaves (Table 1) and soil (Table 2) were in a range from 80-88% and 83-92% respectively.

Table 1

Recovery studies of malathion in lettuce leave samples.

S. No.	Added	Found	Recovery(%)
1.	0.01µg/mL	0.008µg/mL	80
2.	0.0025µg/mL	0.0022µg/mL	88
3.	0.005ng/mL	0.0042ng/mL	84
4.	0.001ng/mL	0.0008ng/mL	84

Table 2

Recovery studies of malathion in soil sample.

S. No.	Added	Found	Recovery(%)
1.	0.01µg/mL	0.0092µg/mL	92
2.	0.0025µg/mL	0.0021µg/mL	84
3.	0.005ng/mL	0.0044ng/mL	88
4.	0.001ng/mL	0.0008ng/mL	83

The fabricated aptasensor has been compared with the previously reported electrochemical biosensors for the detection of malathion (Table 3). The developed APT/SA/CHIT-IO/FTO based aptasensor has shown better detection limit (0.001 ng/ml) and specificity in comparison to

others. Electrochemical nucleic acid sensors are quite sensitive for the detection of genotoxicants including malathion but lack specificity [39]. Furthermore, Acetylcholinesterase (AChE) inhibition based biosensors have applicability only for initial screening of the samples containing organophosphates as these are not specific for a particular organophospahate. APT/SA/CHIT-IO/FTO based aptasensor has reported high specificity and improved detection limit for malathion in comparison to other biomolecule based sensors. However, Bala et al. have reported a colorimetric aptasensor for the detection of malathion with detection limit of 0.06 pM (0.02pg/ml) with response time of about 1 hr [43]. Present work is the first report on electrochemical aptasensor for the detection of malathion within 15 min upto 0.001 ng/ml.

Table 3

Comparison of the proposed aptasensor with other biosensors for the determination of malathion.

Biosensor	Biomolecule immobilized	Sensing Technique	Linear range (ng/mL)	Detection limit (ng/mL)	Response time	Storage stability (Days)	References
AChE[a]-PAn[b]-PPy[c]-	Enzyme	CV	0.009-499.9	0.9	15 min	30	[44]
MWCNTs[d]/GCE[e] AChE-IONPs/c-	Enzyme	DPV	0.033-23.1	0.033	10 min	90	[45]
MWCNTs[f]/ITO[g] AChE-SiSG[h]-	Enzyme	DPV	69.7-1299.9	56.1	4 min	30	[12]
CPE[i] PLaE-CS/AuNPs-GNs[j]/GCE	Enzyme	DPV	0.495-499.9	0.498	10 min	15	[46]
dsCT-DNA-PPy-PVS[k]/ITO	dsDNA	CV	291.6-4999.8	291.6	0.5 min	150	[39]
AChE/PEDOT-MWCNTs[l]/FTO	Enzyme	DPV	0.0000003-330.35	0.0000003	10 min	30	[31]
APT/SA/CHIT-IO/FTO	DNA Aptamer	DPV	0.001-10	0.001	15 min	14	Present study

[a] AChE- acetylcholinesterase.

[b] PAn- polyaniline.

[c] PPy- polypyrrole.

[d] MWCNTs- multi-walled carbon nanotubes.

[e] GCE- glassy carbon electrode.

[f] c-MWCNTs- carboxylated-MWCNTs.

[g] ITO- indium tin oxide.

[h] SiSG- silica sol-gel.

[i] CPE- carbon paste electrode.

[j] PLaE- CS/AuNPs-GNs- plant esterase-chitosan/gold nanoparticles-graphene nanosheets.

[k] dsCT-DNA- PPy-PVS- double stranded *calf thymus* deoxyribonucleic acid entrapped polypyrrole-polyvinyl sulphonate.

[l] PEDOT-MWCNTs- Poly(3,4-ethylenedioxythiophene)- MWCNTs.

4. Conclusions

The CHIT-IO/FTO based aptaelectrode showed the LOD of about 0.001ng/ml for malathion within 20 min. Compared to enzyme based sensors, the developed aptaelectrode exploit the remarkable specificity of recognition elements to develop efficient biosensors allowing the detection of malathion. The applicability of the developed aptasensor was successfully evaluated by determining malathion in the real sample (lettuce leaves and soil sample) with satisfactory recovery results. The aptasensor can be demonstrated to be a very attractive alternative to quantify and examining malathion due to its sensitivity, stability, short analysis time and cost

effectiveness. Further improvement in terms of LOD and real sample recoveries can be done by explored using conducting polymers and other nanomaterial based nanocomposites.

Acknowledgements

We are thankful to Central Instrument Laboratory (CIL) facility of Panjab University (PU), Chandigarh, for FE-SEM, TEM and FT-IR studies. The authors acknowledge University Grant Commission (UGC) Start-Up Grant [F.20-1/2012/BSR/20-7(12/2012], UGC-SAP [F.4-7/2015/DBS-111(SAP-11)], DST-PURSE II, and Department of Biotechnology (DBT)-sponsored project [BT/PR5503/MED/29/642/2012] for funding the work throughout the research. CSIR is also acknowledged for the award of JRF ship.

References

[1]. A. Sassolas, B.P. Simon, J.L. Marty, Biosensors for pesticide detection: New Trends, AJAC 3 (2012) 210-232.

[2]. R. Singh, R. Prasad, G. Sumana, K. Arora, S. Sood, R.K. Gupta, B.D. Malhotra, STD sensor based on nucleic acid functionalized nanostructured polyaniline, Biosens. Bioelectron. 24 (2009) 2232-2238.

[3]. M.R. Bonner, J. Coble, A. Blair, L.E.B. Freeman, J.A. Hoppin, D.P. Sandler, M.C.R. Alavanja, Malathion exposure and the incidence of cancer in the agricultural health study, Am. J. Epidemiol. 166 (2007) 1023-1034.

[4]. W. J. Donarski, D.P. Dumas, D.P. Heitmeyer, V. E. Lewis, F.M. Raushel, Structure- activity relationships in the hydrolysis of substrates by the Phosphortriesterase from Pseudomonas diminuta, Biochemistry 28 (1989) 4650-4655.

[5]. J.M. Abad, F. Pariente, L. Hernandez, H.D. Abruna, E. Lorenzo, Determination of organophosphorous and carbamate pesticides using a piezoelectric biosensor, Anal. Chem. 70 (1998) 2848-2855.

[6]. B. Albero, C.S. Brunete, J.L. Tadeo, Determination of organophosphorus pesticides in fruit juices by matrix solid-phase dispersion and gas chromatography, J. Agric. Food. Chem. 51 (2003) 6915-6921.

[7]. C.C. Leandro, P. Hancock, R.J. Fussell, B.J. Keely, Comparison of ultraperformance liquid chromatography and high-performance liquid chromatography for the determination of priority pesticides in baby foods by tandem quadrupole mass spectrometry, J. Chromatogr. A 1103 (2006) 94-101.

[8]. F. Hernandez, J.V. Sancho, O.J. Pozo, Critical review of the application of liquid chromatography/mass spectrometry to the determination of pesticide residues in biological samples, Anal. Bioanal. Chem. 382 (2005) 934-946.

[9].G. Qian, L. Wang, Y. Wu, Q. Zhang, Q. Sun, Y. Liu, F. Liu, A monoclonal antibody-based sensitive enzyme-linked immunosorbent assay (ELISA) for the analysis of the organophosphorous pesticides chlorpyrifos-methyl in real samples, Food Chem. 117 (2009) 364-370.

[10]. M. L. Lorin, R. Delepee, P. Morin, Simultaneous enantioselective determination of fenamiphos and its two metabolites in soil sample by CE, Electrophoresis 30 (2009) 2931-2939.

[11]. S.B. Mathewa, A.K. Pillai, V.K. Gupta, A rapid spectrophotometric assay of some organophosphorus pesticide residues in vegetable samples, Spectrochim. Acta Part A 67 (2007) 1430-1432.

[12]. P. Raghu, T.M. Reddy, K. Reddaiah, B.E.K. Swami, M. Sreedhar, Acetylecholinestrase based biosensor for monitoring of Malathion and Acephate in food samples: A voltammetric study. Food Chem. 142 (2014) 188-196.

[13]. D. Du, J.W. Ding, J. Cai, A.D. Zhang, One-step electrochemically deposited interface of chitosan-gold nanoparticles for acetylcholinesterase biosensor design, J. Electroanal. Chem. 605 (2007) 53-60.

[14]. N. Kaur, H. Thakur, R. Kumar, N. Prabhakar, An electrochemical sensor modified with poly(3,4-ethylenedioxythiophene)-wrapped multi-walled carbon nanotubes for enzyme inhibition-based determination of organophosphates, Microchim. acta 201, doi: 10.1007/s00604-016-1871-y.

[15]. N. Kaur, H. Thakur, N. Prabhakar, Conducting polymer and multi-walled carbon nanotubes nanocomposites based amperometric biosensor for detection of organophosphate, J. Electroanal. Chem. 2016, doi: 10.1016/j.jelechem.2016.05.037.

[16]. C.L.A. Hamula, J.W. Guthrie, H. Zhang, X. Li, X.C. Le, Selection and analytical applications of aptamers, Trends Anal. Chem. 25 (2006) 681-691.

[17]. T. Mairal, V.C. Ozalp, P.L. Sanchez, M. Mir, I. Katakis, C.K. O'Sullivan, Aptamers: molecular tools for analytical applications, Anal. Bioanal. Chem. 390 (2008) 989-1007.

[18]. O. Shulga, J.R. Kirchhoff, An acetylcholinesterase enzyme electrode stabilized by an electrodeposited gold nanoparticle layer, Electrochem. Commun. 9 (2007) 935-940.

[19]. L. Barthelmebs, A. Hayat, A.W. Limiadi, J.L. Marty, T. Noguer, Electrochemical DNA aptamer-based biosensor for OTA detection, using superparamagnetic nanoparticles, Sens. Actuat. B Chem. 156 (2011) 932-937.

[20] K. Arora, A. Chaubey, R. Singhal, R.P. Singh, S.B. Samanta, S. Chand, B.D. Malhotra, Application of electrochemically prepared polypyrrole-polyvinyl sulphonate films to DNA biosensors, Biosens. Bioelectron. 21 (2006) 1777-1783.

[21]. F. Lucrelli, A. Kicela, G. Palchetti, G. Marrazza, M. Mascini, Electrochemical DNA biosensor for analysis of wastewater samples, Bioelectrochemistry 58 (2002) 113-118.

[22]. A. Hayat, S. Andreescu, J.L. Marty, Design of PEG-aptamer two piece macromolecules as convenient and integrated sensing platform: application to the label free detection of small size molecules, Biosens. Bioelectron. 45 (2013) 168-173.

[23]. L. Shen,Z. Chen, Y. Li, S. He, S. Xie, X. Xu, Z. Liang , X. Meng, Q. Li, Z. Zhu, M. Li, X.C. Le, Y. Shao, Electrochemical DNAzyme sensor for lead based on amplification of DNA-Au bio-bar codes, Anal. Chem. 80 (2008) 6323-6328.

[24]. L. Fan, G. Zhao, H. Shi, M. Liu, Z. Li, A highly selective electrochemical impedance spectroscopy-based aptasensor for sensitive detection of acetamiprid, Biosens. Bioelectron. 43 (2013) 12-18.

[25]. M. Hasanzadeh, A. Bahrami, M. Alizadeh, N. Shadjou, Magnetic nanoparticles loaded on mobile crystalline material-41: preparation, characterization and application as a novel material for the construction of an electrochemical nanosensor, RSC Adv. 3 (2013) 24237-24246.

[26]. A. Kaushik, P.R. Solanki, A.A. Ansari, B.D. Malhotra, S. Ahmad, Iron oxide- chitosan hybrid nanocomposite based nucleic acid sensor for pyrethroid detection, Biochem. Eng. J. 46 (2009) 132-140.

[27]. N. Prabhakar, P.R. Solanki, A. Kaushik, M.K. Pandey, B.D. Malhotra, Peptide nucleic acid immobilized biocompatible silane nanocomposite platform for Mycobacterium tuberculosis detection, Electroanal. 22 (2010) 2672-2682.

[28]. S.P. Singh, S. Arya, P. Pandey,B.D. Malhotra, S. Saha, K. Sreenivas, V. Gupta, Cholestrol biosensor based on rf sputtered zinc oxide nanoporous thin film, App. Phys. Lett. 91 (2007) 063901.

[29]. A. A. Ansari, A. Kaushik, P.R. Solanki, B.D. Malhotra, Sol-gel derived nanoporous cerium oxide film for application to cholesterol biosensor, Electrochem. Commun. 10 (2008) 1246-1249.

[30]. J.K.F. Suh, H.W.T. Matthew, Application of chitosan-based polysaccharide biomaterials in cartilage tissue engineering: a review, Biomaterials 21 (2000) 2589-2598.

[31]. N. Kaur, H. Thakur, N. Prabhakar, Conducting polymer and multi-walled carbon nanotubes nanocomposites based amperometric biosensor for detection of organophosphate, J. Electroanal. Chem. (2016), doi: 10.1016/j.jelechem.2016.05.037.

[32]. F. Barahona, C.L. Bardliving, A. Phifer, J.G. Bruno, C.A. Batt, An aptasensor based on polymer-gold nanoparticle composite microspheres for the detection of Malathion using surface-enhanced raman spectroscopy, Ind. Biotechnol. 9 (2013) 42-50.

[33]. H. Thakur, N. Kaur, N. Prabhakar, Metal oxide nanoparticle-embedded chitosan matrix based electrochemical detection of DNA hybridization, BioNanoSci. 4 (2014) 322-328.

[34]. P. Mallick, B.N. Dash, X-ray diffraction and UV-visible characterizations of α-Fe_2O_3 nanoparticles annealed at different temperature, J Nanosci. Nanotechnol. 3 (2013) 130-134.

[35]. M. Arakha, S. Pal, D. Samantarrai, T.K. Panigrahi, B.C. Mallick, K. Pramanik, B. Mallick, S. Jha, Antimicrobial activity of iron oxide nanoparticle upon modulation of nanoparticle-bacteria interface, Sci. Rep. 5 (2015) 14813.

[36]. F. Tian, Y. Liu, K. Hu, and B. Zhao, The depolymerization mechanism of chitosan by hydrogen peroxide, J. Mater. Sci. 38 (2003) 4709-4712.

[37]. T. Jeyapragasam, R. Saraswathi, Electrochemical biosensing of carbofuran based on acetylcholinesterase immobilized onto iron oxide chitosan nanocomposite, Sens. Actuators B-Chem. 191 (2014) 681-687.

[38]. J. Gunn, S.I. Park, O. Veiseh, O.W. Press, M. Zhang, A pretargeted nanoparticle system for tumor cell labeling, Mol. BioSyst. 7 (2011) 742-748.

[39]. N. Prabhakar, K. Arora, S.P. Singh, M.K. Pandey, H. Singh, B.D. Malhotra, Polypyrrole-Polyvinyl sulphonate film based disposable nucleic acid biosensor, Anal. Chim. Acta 589 (2007) 6-13.

[40]. M. Banyay, M. Sarkar, A. Graslund, A library of IR bands of nucleic acids in solution, Biophys. Chem. 104 (2003) 477-488.

[41]. G. Zhao, J.J. Xu, H.Y. Chen, Fabrication and characterization of iron oxide multilayer film and its application in promoting direct electron transfer of haemoglobin. Electrochem. Commun.8 (2006) 148-154.

[42]. A.S. Esfahni, M.T. Salehi, M.N. Esfahni, E. Ekramian, Chitosan-modified superparamgnetic iron oxide nanoparticles: design, fabrication, characterization and antibacterial activity, CHEMIK 69 (2015) 19-32.

[43]. R. Bala, M. Kumar, K. Bansal, R.K. Sharma, N. Wangoo, Ultrasensitive aptamer biosensor for malathion detection based on cationic polymer and gold nanoparticles, Biosens. Bioelectron. 85 (2016) 445-449.

[44]. D. Du, X. Ye, J. cai, J. Liu, A. Zhang, Acetylcholinesterase biosensor design based on carbon nanotube-encapsulated polypyrrole and polyaniline copolymer for amperometric detection of organophosphates, Biosens. Bioelectron. 25 (2010) 2503-2508.

[45]. N. Chauhan, C.S. Pundir, An amperometric acetylecholinestrase sensor based on Fe_3O_4 nanoparticle/ multi-walled carbon nanotube-modified ITO-coated glass plate for the detection of pesticides, Electrochim. Acta 67 (2012) 79-86.

[46]. J. Bao, C. Hou, M. Chen, J. Li, D. Huo, M. Yang, X. Luo, Y. Lei, Plant esterase-chitosan/gold nanoparticles-graphene nanosheet composite-based biosensor for the ultrasensitive detection of organophosphate pesticides, J. Agric. Food Chem. 63 (2015) 10319-10326.

Figure Captions:

Scheme. 1. Schematic illustration for the fabrication of working aptaelectrode.

Fig. 1. Characterization studies of Iron oxide nanoparticles: **(A)** TEM image, **(B)** UV-visible spectra.

Fig. 2. FT-IR images (a) CHIT/FTO (b) CHIT-IO/FTO (c) SA/CHIT-IO/FTO (d) APT/SA /CHIT-IO/FTO.

Fig. 3. FE-SEM images **(A)** CHIT/FTO **(B)** CHIT-IO/FTO **(C)** SA/CHIT-IO/FTO **(D)** APT/SA/ CHIT-IO/FTO.

Fig. 4. (A) DPV studies of i) CHIT/FTO ii) CHIT-IO/FTO iii) SA/CHIT-IO/FTO iv) APT/SA/CHIT-IO/FTO v) MAL/APT/SA/CHIT-IO/FTO at potential range from 0.2 to 0.6 V, in

0.05M PBS (pH-7.0, 0.9% NaCl) containing 5mM $[Fe(CN_6)]^{3-/4-}$ and **(B)** EIS measurements of i) CHIT/FTO ii) CHIT-IO/FTO iii) SA/CHIT-IO/FTO iv)APT/SA/CHIT-IO/FTO v) MAL/APT/SA/CHIT-IO/FTO in 0.05M PBS (pH-7.0, 0.9% NaCl) containing5mM $[Fe(CN_6)]^{3-/4-}$ within the frequency range 100 kHz-100 mHz.

Fig. 5. DPV response of **(A)** aptaelectrode with different concentrations of malathion (a) Bare aptaelectrode (b) 0.001ng/mL (c) 0.005ng/mL (d) 0.0001µg/mL (e) 0.001µg/mL (f) 0.0025µg/mL (g) 0.01µg/mL; at potential range from 0.2 – 0.7 V, in 0.05 M PBS (pH-7.0, 0.9% NaCl) containing 5mM $[Fe(CN)_6]^{3-/4-}$ and **(B)** shows the linear relationship between the peak current changes obtained by DPV and the logarithm of malathion concentrations. Error bars show the standard deviations of measurements taken from three independent experiments.

Fig. 6. DPV studies to evaluate (**A)** Stability of aptaelectrode with malathion a) 0 day b) 14 day c) 21 day d) 28 day; and **(B)** Regeneration with 50mM NaOH (a) Aptelectrode (b) Reg 1 (c) Reg 2 (d) Reg 3 (e) Reg 4 (f) Reg 5 (g) Reg 6 (h) Reg 7; at potential range from 0.1 -0.8 V , in 0.05 M PBS (pH-7, 0.9% NaCl) containing 5mM $[Fe(CN)_6]^{3-/4-}$.

Highlights

- An electrochemical aptasensor for the detection of Malathion has been developed.
- Chitosan-iron oxide NP deposited FTO sheets provides platform for aptamer immobilization.
- Aptasensor has efficiency to detect malathion upto 0.001ng/mL within 15 min